Journal Pre-proof

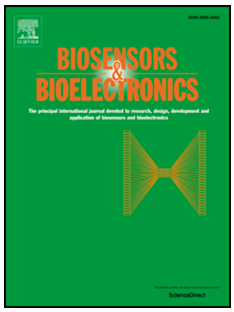

Two-dimensional membrane scaffold for the oriented immobilization of biosensing molecules

Masumi Iijima, Tsutomu Nakayama, Shun'ichi Kuroda

PII: S0956-5663(19)30939-X

DOI: https://doi.org/10.1016/j.bios.2019.111860

Reference: BIOS 111860

To appear in: *Biosensors and Bioelectronics*

Received Date: 9 September 2019

Revised Date: 21 October 2019

Accepted Date: 7 November 2019

Please cite this article as: Iijima, M., Nakayama, T., Kuroda, Shun'., Two-dimensional membrane scaffold for the oriented immobilization of biosensing molecules, *Biosensors and Bioelectronics* (2019), doi: https://doi.org/10.1016/j.bios.2019.111860.

(*Biosensors and Bioelectronics, Research Article*)

Two-dimensional membrane scaffold for the oriented immobilization of biosensing molecules

Masumi Iijima[a,b], Tsutomu Nakayama[b], Shun'ichi Kuroda[a,*]

[a] The Institute of Scientific and Industrial Research, Osaka University, Ibaraki, Osaka 567-0047, Japan

[b] Department of Nutritional Science and Food Safety, Faculty of Applied Bioscience, Tokyo University of Agriculture, Setagaya, Tokyo 156-8502, Japan

(For footnotes)

*Corresponding author: Tel.: +81-6-6879-8460; fax: +81-6-6879-8464.

Email address: skuroda@sanken.osaka-u.ac.jp (S. Kuroda).

ABSTRACT

The orientation and density of biosensing molecules on sensor chip should be precisely controlled to improve sensitivity and ligand-binding capacity. We previously developed a ~30-nm bio-nanocapsule (ZZ-BNC), consisting of the hepatitis B virus envelope L protein fused with the tandem form of protein A-derived IgG Fc-binding Z domain (ZZ-L protein). This is used as a robust nanoparticle scaffold to enhance the sensitivity and ligand-binding capacity of IgGs and Fc-fused sensing molecules (Fc-fused receptors). However, due to their rigid particle structure, the surface density of ZZ-L proteins could not be optimized for biosensor functions, and useless ZZ-L proteins become stuck between ZZ-BNC and the sensor chip. Here, we have developed a planar lipid membrane embedded with ZZ-L micelles (ZZ-L membrane), which could modify the surface of any biosensor chip with a controlled density of ZZ-L proteins. Compared with ZZ-BNC, the sensitivity and ligand-binding capacity of IgGs were enhanced about 10-fold with the ZZ-L membrane. Furthermore, the immobilized IgGs could capture their respective antigens almost stoichiometrically, indicating that ZZ-L membrane is the most ideal scaffold for Fc-fused sensing molecules in terms of both clustering and oriented immobilization.

Keywords

Two-dimensional membrane, Scaffold, Bio-nanocapsule, Oriented immobilization, Sensing molecule

1. Introduction

The oriented immobilization of sensing molecules on the surface of a biosensor chip is critical for improving the sensitivity, specificity, ligand-binding capacity, and avidity of biosensors. Conventionally, various scaffolds (*e.g.*, crosslinkers/polymers (Mandenius et al., 1984), self-assembled monolayers (SAMs) (Mirsky et al., 1997), an IgG Fc-binding protein A/G or peptide (Davis and Leary 1989), DNA (Niemeyer et al., 1994), and a biotin/(strept)avidin complex (Updyke and Nicolson 1984)) have all been utilized as immobilizing sensing molecules on the biosensor chip (Iijima and Kuroda, 2017). The essential requirements for scaffolds are as follows: 1) scaffolds should tether sensing molecules in a non-destructive binding mode; 2) scaffolds should tether sensing molecules through specific residues without increasing steric hindrance around the ligand-biding site; 3) scaffolds should be fixed on the biosensor chip in an oriented immobilization manner; 4) scaffolds should possess rigid linkers for repressing the excess fluctuation of the sensing molecule; and 5) scaffolds should have a robust structure for repetitive use. However, so far, no conventional scaffolds fulfilled all of these requirements concurrently is in use.

Bio-nanocapsule (BNC) is a hepatitis B virus subviral particle composed of envelope L proteins and a lipid bilayer membrane, which can be efficiently synthesized in the recombinant yeast *Saccharomyces cerevisiae* (Kuroda et al., 1992; Jung et al., 2011). We have modified L protein by replacing its N-terminal region with a tandem form of protein A-derived IgG Fc-binding Z domain to generate the ZZ-L protein, which can be synthesized in yeast as particles of approximately 30 nm (designated as ZZ-BNCs) (*see* Fig. 1A). Since ZZ-BNC deploys the ZZ domain outwardly in a rigid form, it could spontaneously tether the Fc regions of IgGs without chemical

modification in an oriented immobilization manner, and thereby display all Fv regions radially for efficient antigen binding (Iijima et al., 2011a; 2012). When IgGs and Fc-fused receptors were used as sensing molecules for quartz crystal microbalance (QCM) and surface plasmon resonance (SPR), the ZZ-BNC-coated biosensor chip markedly enhanced the sensitivity, ligand-binding capacity, and avidity compared to the bare sensor chip (Iijima and Kuroda, 2017). Furthermore, the ZZ-BNC structure is applicable for various detection methods (enzyme-linked immunosorbent assay (ELISA), western blot analysis, and fluorophore-linked immunosorbent assay (FIA)) (Iijima et al., 2010; 2011b, 2013a; 2013b; 2016). Thus, ZZ-BNC was revealed to fulfill the aforementioned essential requirements for scaffolds.

Since ZZ-BNC possesses rigid particle structure, and the surface density of ZZ-L proteins is already determined upon their biosynthesis in yeast cells (*i.e.*, ~120 molecules/ZZ-BNC; ~4.25 × 10^{-2} molecules/nm^2 (Iijima et al., 2012)), the surface density of ZZ-L proteins could not be optimized for biosensor functions. In theory, a higher density of ZZ-L proteins would increase the steric hindrance around the antigen-recognition sites of IgGs, lower density of ZZ-L proteins would decrease the sensitivity and antigen-binding capacity of biosensors. Furthermore, since ZZ-BNC possesses robust particle structure (Yamada et al., 2001)), ZZ-L proteins stuck between ZZ-BNC and the biosensor chip could not participate in the tethering of IgGs. In this study, we investigated the disassembly conditions for ZZ-BNC (formation of ZZ-L micelles (ZZ-L-Mic)) and the assembly conditions for ZZ-L membrane (ZZ-L-Mem, membrane embedded with ZZ-L-Mic) (*see* Fig. 1B). We applied ZZ-L-Mem to biosensor chips to optimize the surface density of ZZ-L proteins and reduce the amount of useless ZZ-L proteins.

2. Materials and methods

2.1. ZZ-BNC and ZZ-L-Mic

ZZ-BNCs were overexpressed in *Saccharomyces cerevisiae* AH22R^{-} cells carrying the ZZ-L-expression plasmid pGLD-ZZ50 (Iijima et al., 2011a). ZZ-L proteins were synthesized as a transmembrane protein in the endoplasmic reticulum, and formed ~30 nm particles (ZZ-BNCs) spontaneously in the lumen (Kuroda et al., 1992). ZZ-BNCs were extracted from yeast cells by disruption with glass beads, followed by heat treatment at 70 °C for 20 min to remove yeast-derived protein, and purified using an AKTA™ (GE Healthcare, Amersham, UK) by porcine IgG-immobilized affinity chromatography and size exclusion chromatography as previously described (Jung et al., 2011; Iijima et al., 2011a). Each ZZ-BNC contains approximately 120 molecules of ZZ-L protein, deploying ZZ domains outwardly on its surface (Iijima et al., 2011a). ZZ-L-Mic (ZZ-L protein embedded in a micelle) was prepared from ZZ-BNCs by vortexing with 5% (w/v) Tween 80 at room temperature for 1 min and subsequently incubating at room temperature for 30 min.

2.2. Reagents

The detergents used in the preparation of ZZ-L-Mic were as follows: *n*-Octyl-β-D-glucopyranoside (OG, Dojindo (Kumamoto, Japan)); polyoxyethylene sorbitan monolaurate (Tween 20, Nacalai Tesque (Kyoto, Japan)); polyethylene glycol nonylphenyl ether (NP40, Nacalai Tesque); polyoxyethylene sorbitan monooleate (Tween 80, FUJIFILM Wako Pure Chemical Corporation (Osaka, Japan)); phase-transfer surfactant Cell-LyEX-MP (Toyo Ink group (Tokyo, Japan)); sodium dodecyl sulfate (SDS, Sigma–Aldrich (Saint Louis, MO, USA));

4-(1,1,3,3-tetramethylbutyl)phenyl-polyethylene glycol (Triton X-100, Sigma–Aldrich); (1,1,3,3-tetramethylbutyl)phenyl-polyethylene glycol (Triton X-114, Sigma–Aldrich); 3-[(3-cholamidopropyl)dimethylammonio]-1-propanesulfonate hydrate (CHAPS, Sigma–Aldrich); and N,N-dimethyldodecylamine N-oxide (LDAO, Sigma–Aldrich). Rabbit total IgGs, anti-actin mouse IgG2a, anti-chicken IgY rabbit polyclonal IgG, and actin were purchased from Sigma–Aldrich. Chicken IgY was from R&D Systems (Minneapolis, MN, USA). Block Ace powder was purchased from DS Pharma Biomedical Co. Ltd. (Osaka, Japan). Dioleyl phosphatidylcholine (DOPC) was obtained from NOF Corporation (Tokyo, Japan).

2.3. Lipid-bilayer (LB) membranes and ZZ-L-Mem

DOPC dissolved in chloroform/methanol (2:1, volume) was added to a round bottom flask, evaporated to form a thin film, and hydrated with 10 mM Tris-HCl buffer (pH 8.0) to obtain liposomes. This was followed by sonication in a bath-type sonicator. The liposome size was trimmed by extrusion with a 50 or 100 nm polycarbonate membrane to form 100 nm liposomes. LB membrane was prepared by contacting DOPC liposomes (1 µg) with mica substrate (1 cm^2, Ted Pella, Inc., Redding, CA, USA) at room temperature for 30 min. Subsequently, ZZ-L-Mic (0.01 µg as ZZ-L protein) was contacted with the LB membrane, and then incubated at room temperature for 30 min to obtain ZZ-L-Mem.

2.4. Atomic force microscopy (AFM)

Three microliters of ZZ-BNC, ZZ-L-Mic, and ZZ-L-Mem (0.01 mg/mL as ZZ-L protein) were spotted onto the mica substrate, incubated at room temperature for

30 min, and washed with distilled water. After drying in air, surface topographical images of the fabricated mica substrate were obtained using atomic force microscopy (AFM) (model SPA-400; Hitachi High-Tech Science Corporation, Tokyo, Japan). Raw AFM images were taken in non-contact mode in air at room temperature. The scanning rate was modulated to 1 Hz for a 300 × 300 nm scale image.

2.5. Transmission electron microscopy (TEM)

ZZ-BNCs or ZZ-L-Mem (0.01 µg as protein) were mixed with 10-nm gold particle-labeled goat total IgG (5 µL, Sigma-Aldrich). They were adsorbed onto a carbon-coated copper grid (JEOL, Tokyo, Japan), negatively stained using 2% (w/v) phosphotungstic acid (pH 7.0), and subjected to TEM using model JEM1011 (JEOL).

2.6. Quartz crystal microbalance (QCM)

QCM analysis was performed with a QCM model Twin-Q (As One Corp., Osaka, Japan) as previously described (Iijima et al., 2011a). Briefly, the QCM sensor chip (9-mm diameter Au disk) was washed with piranha solution (1:3 (v/v) H_2O_2:H_2SO_4), rinsed with distilled water, and then treated with ZZ-BNCs (1 µg/mL as ZZ-L protein) or ZZ-L-Mem (1 µg/mL as ZZ-L protein) in phosphate-buffered saline [PBS: 137 mM NaCl, 2.7 mM KCl, 10 mM Na_2PO_4, 2 mM KH_2PO_4, pH 7.4]) at 25°C. ZZ-BNC-coated and ZZ-L-Mem-coated sensor chips were blocked with PBS containing 5% (w/v) Block Ace powder. Subsequently, IgGs (7.2-23.6 µg/mL, final concentration) were immobilized onto each sensor chip. As a control, bare sensor chips were contacted with the same concentrations of IgGs and blocked similarly. After the addition of antigens (0-35.7 µg/mL, final concentration), when a stable frequency (less than ± 3 Hz)

was observed for >1 min, the protein–protein interactions were judged to be equilibrated. These measurements were repeated at least 3 times. A frequency change (ΔF) of 1 Hz corresponded to a weight change of 0.6 ng/cm^2 (as calculated by the Sauerbrey equation) (Sauerbrey, 1959). While the limit of detection (LOD) of this QCM equipment was indicated as ΔF of 3.3 Hz (corresponding to 2 ng/cm^2), we used ΔF of 5.0 Hz (corresponding to 3 ng/cm^2) as the LOD for increasing reliability.

2.7. Surface plasmon resonance (SPR)

SPR measurements were performed with an automated SPR-based instrument for biomolecular interaction analyses (Biacore T200; GE Healthcare). Briefly, after adsorption of ZZ-BNCs (5 µg/mL as ZZ-L protein, flow cell 3) or ZZ-L-Mem (5 µg/mL as ZZ-L protein, flow cell 4) onto the Au sensor chip using PBS (flow rate, 10 µL/min; 10 min), both sensor chips were blocked with PBS containing 5% (w/v) Block Ace powder. Anti-chicken IgY (2.5 µg/mL) was immobilized onto ZZ-BNC-coated (flow cell 3) or ZZ-L-Mem-coated (flow cell 4) Au sensor chips using PBS (flow rate, 5 µL/min; 18 min). As a control, bare sensor chips (flow cell 2) were contacted with anti-chicken IgY (2.5 µg/mL) and blocked similarly. Subsequently, all sensor chips were subjected to the interaction analysis with chicken IgY (0-500 nM; flow rate, 30 µL/min; 3 min). The dissociation phase was then monitored for 10 min. A buffer blank injection (flow cell 1) was performed for double referencing. Assay data files were analyzed with BiaEvaluation Software 4.1 (GE Healthcare). To determine the kinetic rate constant for association and dissociation, the simple 1:1 kinetic model was fitted to each dataset with terms for the on-rate constant (k_a) and off-rate constant (k_d). These kinetic constants were fitted globally for each assay set.

3. **Results and discussion**

3.1. Preparation of ZZ-L micelles (ZZ-L-Mic)

ZZ-BNC is a liposome embedded with ~60 molecules of the ZZ-L protein dimer (*i.e.*, ~120 molecules of ZZ-L protein monomer). More than 90% (w/w) of BNCs were found to retain their particle structure after heat treatment (at 80°C for 5 min), 0.2% (w/v) SDS treatment (at room temperature for 30 min), acid/alkaline treatment (pH 2-12, at 25°C for 20 min) (Yamada et al., 2001; Iijima et al., 2011a), or sonication (unpublished data). We therefore treated ZZ-BNCs with higher concentration of various detergents (*e.g.*, 5% (w/v) of LyEX-MP, NP40, OG, Tween 20, Tween 80, SDS, Triton X-100, Triton X-114, CHAPS, and LDAO) at room temperature for 30 min, and then observed them under AFM. As shown in Fig. 2A, the typical dome shape of ZZ-BNCs (~12.7 ± 0.7 nm in height, ~38.0 ± 3.0 nm in diameter) was eliminated only by 5% Tween 80 treatment, not by other detergents. The dome shape of ZZ-BNCs was not affected by treatments of less than 4% Tween 80, while the ZZ-BNCs were transformed to small elliptical granules (~2.3 ± 0.2 nm in height, ~6.5 ± 0.8 nm in short diameter, ~9.4 ± 1.5 nm in long diameter) by 5% Tween 80 treatment (Fig. 2B). Based on the high-speed AFM observation of the ZZ-BNC surface (Iijima et al., 2012), the cross section of ZZ-L protein homodimers (consisting of two cylindrical ZZ-L protein monomers) is two connected ellipses of ~4.7 ± 1.4 nm in short diameter and ~7.0 ± 2.0 nm in long diameter. Thus, each small elliptical granule was considered to be micelles containing the ZZ-L protein homodimer (designated as ZZ-L micelles (ZZ-L-Mic); Fig. 2C). Since the critical micelle concentration (CMC) of Tween 80 (0.0015 mM (Mahmood and Al-Koofee, 2013)) is lowest of all the detergents, Tween 80 may be most suitable for disrupting the membrane portion of ZZ-BNCs to form small micelles

containing ZZ-L proteins. Finally, 5% Tween 80 treatment was used for further preparation of ZZ-L-Mic.

3.2. Preparation of ZZ-L membrane (ZZ-L-Mem)

Formation of the ZZ-L membrane (ZZ-L-Mem) was examined by contacting ZZ-L-Mic with a lipid-bilayer (LB) membrane (*see* Fig. 1B). LB membrane (100% DOPC) on mica substrate was incubated with ZZ-L-Mic at room temperature for 30 min. Under AFM observation in air, the height and roughness were changed from ~5.5 ± 1.1 nm and ~0.2 ± 0.0 nm to ~7.4 ± 1.2 nm and ~1.6 ± 0.1 nm, respectively (Fig. 3A). Based on the observed shape of the ZZ-L-Mic (*see* Fig. 2C), ZZ-L-Mic may be adsorbed onto the LB membrane efficiently and transformed to dome-shaped structure. When the same amount of ZZ-L protein was used, the ZZ-L-Mem on mica substrate showed a smooth dome shape (~7.4 ± 1.2 nm in height, ~65.0 ± 4.9 nm in diameter, ~1.6 ± 0.1 nm in roughness; Fig. 3B, lower panels), while ZZ-BNCs on mica substrate exhibited a relatively rugged dome shape (~12.7 ± 0.7 nm in height, ~38.0 ± 3.0 nm in diameter, ~2.1 ± 0.1 nm in roughness; Fig. 3B, upper panels). The difference in height between ZZ-L-Mem and ZZ-BNC might be attributed to the number of bilayer membranes (*i.e.*, one for ZZ-L-Mem, two for ZZ-BNC). It was shown that useless ZZ-L proteins stuck under ZZ-BNC were eliminated by transforming to ZZ-L-Mem. The coverage rate of ZZ-L proteins was estimated to increase about 3.0 fold, indicating that the density of ZZ-L protein could be optimized by changing the ratio of ZZ-L-Mic to LB membrane. Next, ZZ-BNC and ZZ-L-Mem (0.01 µg as ZZ-L protein) were mixed with or without 10-nm gold particle-labeled goat total IgG, adsorbed onto carbon-coated copper grid, stained negatively, and then observed under TEM (Fig. 3C). ZZ-BNCs

exhibited relatively uniform particle structure (~28.3 ± 1.9 nm (n = 10) in diameter), which were surrounded coronally by 10-nm gold-labeled IgGs (Fig. 3C, upper panels). By the formation of ZZ-L-Mem, ZZ-L proteins lost their typical particle structure and formed small granules (~10.9 ± 1.2 nm (n = 10) in diameter), but retained comparable level of IgG-binding capacity on the whole surface (Fig. 3C, middle panels). While the particle structure of ZZ-BNC was disrupted, ZZ-L-Mic may be successfully embedded in LB membrane with deploying ZZ domains upwards, corroborating our membrane-orientation model for ZZ-L-Mem (Fig. 3B, lower panels).

3.3. Optimization of ZZ-L-Mem-coated sensor chips for QCM

ZZ-L-Mem was applied to the QCM analysis using α-actin mouse IgG2a to detect actin. ZZ-L-Mem consisting of LB membrane (315 ng/cm^2) and various amounts of ZZ-L protein (0-1250 ng/cm^2) were used to immobilize α-actin IgG on the sensor chip (Fig. 4A). The amount of immobilized α-actin IgG increased in proportion to the amount of ZZ-L protein. Subsequently, actin was contacted with each sensor chip to measure the maximum actin-binding capacity (Fig. 4B). It was found that ~750 ng/cm^2 of ZZ-L protein could allow for the most effective binding of actin. However, >800 ng/cm^2 of ZZ-L protein did not show comparable levels of actin binding, suggesting that the interaction of actin with α-actin IgGs is suppressed by the steric hindrance caused by the over-packing of α-actin IgGs on ZZ-L-Mem. When the number of bound actin was divided by the number of immobilized α-actin IgG, 1.0 mol of IgG at ~750 ng/cm^2 of ZZ-L protein could bind ~2.0 ± 0.4 mol of actin (Fig. 4C), which was comparable to the theoretical maximum binding capacity. In the case of ZZ-BNCs, 1.0 mol of IgG at ~750 ng/cm^2 of ZZ-L protein could bind only ~1.2 ± 0.2 mol of actin (Iijima et al., 2011a). It

was confirmed that ZZ-L-Mem could optimize the density of the ZZ-L protein to maximize the antigen-binding capacity of IgGs.

3.4. Robustness of ZZ-L-Mem-coated sensor chips

Since ZZ-BNC was shown to exhibit outstanding robustness, the ZZ-BNC-coated Au sensor chip could be used repeatedly, more than 20 times in QCM (Iijima et al., 2011a). To evaluate the robustness of ZZ-L-Mem-coated sensor chips, the chip was subjected to a repetitive antibody adsorption/removal process, such as blocking with Block Ace, incubation with rabbit total IgG for 3 min, washing twice with 0.16 N HCl to strip bound IgG, and washing three times with PBS. This cycle of adsorption and antibody removal was repeated 20 times to the same ZZ-L-Mem (Fig. 4D). The frequency change (ΔF) observed in the 20th cycle was >85% of the ΔF observed in the first cycle. Thus, ZZ-L-Mem adsorbed onto the Au surface of a sensor chip was stable, presumably by forming Au–S covalent linkages with some of the 14 Cys residues in the ZZ-L protein.

3.5. Effect of ZZ-L-Mem on QCM analysis

To compare ZZ-L-Mem with ZZ-BNC, the gold surface of the QCM sensor chip was treated with ZZ-BNC or ZZ-L-Mem (1 μg/mL as ZZ-L protein). Bare, ZZ-BNC-coated, and ZZ-L-Mem-coated sensor chips (Fig. 5A) were treated with α-actin mouse IgG2a (7.2 μg/mL) or α-chicken IgY rabbit polyclonal IgG (23.6 μg/mL), and then allowed to react with actin or chicken IgY, respectively. The approximate straight line between injected and bound antigens of each sensor chip was shown in Figs. 5B and 5C. Since the QCM equipment has a limit of detection (LOD) of a weight

change of 3 ng/cm^2 (corresponding to ΔF of 5.0 Hz), the lowest concentrations of actin necessary to reach the LOD in bare, ZZ-BNC-coated, and ZZ-L-Mem-coated sensor chips were ~11.0, ~4.49, and ~0.56 μg/mL, respectively (Fig. 5B), indicating that the sensitivity of ZZ-L-Mem-coated sensor chip increased ~19.6-fold compared to the bare sensor chip and ~8.0-fold compared to ZZ-BNC-coated sensor chip. Similarly, the lowest concentrations of chicken IgY necessary to give LOD were ~0.27, ~0.022, and ~0.0004 μg/mL, respectively (the ZZ-L-Mem-coated sensor chip showed ~675-fold increase compared to the bare sensor chip and a ~55-fold increase compared to the ZZ-BNC-coated sensor chip) (Fig. 5C). Thus, by adsorbing antibodies onto the ZZ-L-Mem-coated sensor chip, the sensitivity was dramatically increased in all cases. Next, the antigen-binding capacity of each sensor chip was compared in terms of the upper limit of antigen binding (calculated from maximum ΔF). As shown in Fig. 5B, the amounts of bound actin were ~12.2, ~145.8, and ~903.4 ng/cm^2 for bare, ZZ-BNC-coated, and ZZ-L-Mem-coated sensor chips, respectively. The ZZ-L-Mem-coated sensor chip showed ~74.1-fold and a ~6.2-fold increase compared to bare and ZZ-BNC-coated sensor chip, respectively. Similarly, the amounts of bound chicken IgY were ~50.3, ~288.2, and ~2210.5 ng/cm^2 for bare, ZZ-BNC-coated, and ZZ-L-Mem-coated sensor chips, respectively (Fig. 5C). ZZ-L-Mem-coated sensor chip showed ~43.9-fold and ~7.7-fold increase compared to the bare and ZZ-BNC-coated sensor chips, respectively. Thus, it was demonstrated that the ZZ-L-Mem-coated sensor chip could bind larger amounts of antigens than bare and ZZ-BNC-coated sensor chips. Consequently, the ZZ-L-Mem-coated sensor chip significantly expanded the dynamic concentration ranges of antigens (~1.7–19.7 μg/mL for actin, ~0.0022–2.22 μg/mL for chicken IgY).

Moreover, we evaluated what number of antigens could be bound with one IgG on the bare, ZZ-BNC-coated, and ZZ-L-Mem-coated sensor chips. As shown in Fig. 5D, 1 mol of α-actin IgG in the ZZ-L-Mem-coated sensor chip could bind to 1.75 ± 0.07 mol of actin, while α-actin IgG on the bare and ZZ-BNC-coated sensor chips to 0.03 ± 0.01 mol and 0.76 ± 0.06 mol of actin (~58.4-fold and ~2.3-fold enhancement), respectively. Similarly, 1 mol of the α-chicken IgY rabbit IgG in ZZ-L-Mem-coated sensor chip could bind to 2.17 ± 0.29 mol of chicken IgY, while α-chicken IgY rabbit IgG in bare and ZZ-BNC-coated sensor chips to 0.07 ± 0.04 mol and 1.68 ± 0.10 mol of chicken IgY (~30.3-fold and ~1.3-fold enhancement), respectively. These results indicated that ZZ-L-Mem could function as an ideal scaffold for IgGs, bringing out the theoretical maximum antigen-binding capacity (*i.e.*, ~2 mol of antigens to ~1 mol of IgG).

3.6. Effect of ZZ-L-Mem on SPR analysis

To evaluate the effect of ZZ-L-Mem on the interaction of α-chicken IgY and chicken IgY, we performed kinetics analysis by SPR equipped with bare, ZZ-BNC-coated, and ZZ-L-Mem-coated sensor chips (Fig. 6A). The kinetic interaction of chicken IgY for α-chicken IgY (K_D) was of a higher affinity when analyzed on a ZZ-L-Mem-coated sensor chip (8.78×10^{-13} M) compared to that on a bare sensor chip (6.58×10^{-10} M) or the ZZ-BNC-coated sensor chip (1.24×10^{-11} M) (Fig. 6B). While all sensor chips showed nearly identical on-rate constants (k_a) of these interactions, the off-rate constants (k_d) exhibited a slower dissociation from the ZZ-L-Mem-coated sensor chip (1.31×10^{-7} s^{-1}) when compared with a bare sensor chip (6.65×10^{-5} s^{-1}) and ZZ-BNC-coated sensor chip (1.78×10^{-6} s^{-1}). The ZZ-L-Mem-coated sensor chip was

indicated to reduce the dissociation rates of antigens from antibodies. It was strongly suggested that the steric hindrance around the antigen-binding sites decreased more efficiently with the oriented immobilization of IgG on ZZ-L-Mem rather than the bare and ZZ-BNC, thereby stabilizing the antigen-antibody complexes.

4. Conclusions

To improve biosensors, we have developed ZZ-BNC which could achieve both clustering and oriented immobilization of biosensing molecules on sensor chips. It was demonstrated that ZZ-BNC fulfills five essential requirements for ideal scaffolds (*see* **Introduction**). However, useless ZZ-L proteins are stuck between ZZ-BNC and the sensor chip, and the surface density of ZZ-L proteins could not be optimized to reduce the steric hindrance around the ligand-binding domains of the sensing molecules. In this study, we succeeded in the disassembly of ZZ-BNC (formation of ZZ-L-Mic) and the assembly ZZ-L-Mem (formation of a ZZ-L-Mic-embedded membrane). ZZ-L-Mem could facilitate the optimization of ZZ-L protein density, thereby maximizing the antigen-binding capacity of IgGs (*i.e.*, two mol of antigens bound to one mole of IgG). ZZ-L-Mem also showed excellent robustness comparable to ZZ-BNC. These data indicate that ZZ-L-Mem is the most ideal scaffold for the clustering and oriented immobilization of IgGs (including Fc-fused receptors (Iijima et al., 2016)), applicable to various shapes of biosensor surfaces. So far, the transmembrane domain of outer membrane protein A from *Escherichia coli* (OmpA) has been used as a scaffold for clustering and oriented immobilization of IgGs (Le Brun et al., 2011). ZZ domain-fused OmpA was embedded in self-assembly monolayers (SAMs), which allowed one IgG molecule bound to at most ~0.5 antigen molecules. Although the concept of OmpA is similar to ZZ-L-Mem, OmpA may not sufficiently fulfill the aforementioned five essential requirements for ideal scaffolds, most likely due to excess fluctuation of IgGs. SAM may not stabilize the orientation of OmpA sufficiently, or the linker between the ZZ domain and OmpA may be too flexible in structure.

Acknowledgments

This work was supported in part by KAKENHI (Grant-in-Aid for Scientific Research (S, 16H06314, and A, 18H03938, to SK; C, 16K04888 and 19K05219, to MI), the Japan Agency for Medical Research and Development (17cm0106214h0002 , 17fk0310105h0001, to S.K.), and "Dynamic Alliance for Open Innovation Bridging Human, Environment and Materials" from the Ministry of Education, Culture, Sports, Science and Technology of Japan (MEXT, to S.K.).

References

Davis, K.A. and Leary, T.R., 1989. Anal. Chem. 61, 1227–1230.

Iijima, M., Matsuzaki, T., Kadoya, H., Hatahira, S., Hiramatsu, S., Jung, G., Tanizawa, K., Kuroda, S., 2010. Anal. Biochem. 396, 257–261.

Iijima, M., Kadoya, H., Hatahira, S., Hiramatsu, S., Jung, G., Martin, A., Quinn, J., Jung, J., Jeong, S.Y., Choi, E.K., Arakawa, T., Hinako, F., Kusunoki, M., Yoshimoto, N., Niimi, T., Tanizawa, K., Kuroda, S., 2011a. Biomaterials 32, 1455–1464.

Iijima, M., Matsuzaki, T., Yoshimoto, N., Niimi, T., Tanizawa, K., Kuroda, S., 2011b. Biomaterials 32, 9011–9020.

Iijima, M., Somiya, M., Yoshimoto, N., Niimi, T., Kuroda, S., 2012. Sci. Rep. 2, 790.

Iijima, M., Yamamoto, M., Yoshimoto, N., Niimi, T., Kuroda, S., 2013a. Biosci. Biotechnol. Biochem. 77, 843–836.

Iijima, M., Yoshimoto, N., Niimi, T., Maturana, A.D., Kuroda, S., 2013b. Analyst 138, 3470–3477.

Iijima, M., Yoshimoto, N., Niimi, T., Maturana, A.D., Kuroda, S., 2016. Biotech. J. 11, 805–813.

Iijima, M. and Kuroda, S., Scaffolds for oriented and close-packed immobilization of immunoglobulins. Biosens. Bioelectron., 2017, 89, 810-821.

Jung, J., Iijima, M., Yoshimoto, N., Sasaki, M., Niimi, T., Tatematsu, K., Jeong, S.Y., Choi, E.K., Tanizawa, K., Kuroda, S., 2011. Protein Expr. Purif. 78, 149–155.

Kuroda, S., Otaka, S., Miyazaki, T., Nakao, M., Fujisawa, Y., 1992. J. Biol. Chem. 267, 1953–1961.

Le Brun, A.P., Holt, S.A., Shah, D.S., Majkrzak, C.F., Lakey, J.H., 2011. Biomaterials 32, 3303–3311.

1 Mahmood, M.E. and Al-Koofee, D.A.F. 2013. Global Journal of Science Frontier
2 Research Chemistry 13, 1–7.
3 Mandenius, C.F., Welin, S., Danielsson, B., Lundström, I., Mosbach, K., 1984. Anal.
4 Biochem. 137, 106–114.
5 Mirsky, V.M., Riepl, M., Wolfbeis, O.S., 1997. Biosens. Bioelectron. 12, 977–989.
6 Niemeyer, C.M., Sano T, Smith CL, Cantor CR., 1994. Nucleic Acids Res. 22, 5530–
7 5539.
8 Sauerbrey, G. Z., 1959. Zeitschrift für Physik 155, 206−222.
9 Shin, S.H., Jeong, S.Y., Choi, E.K., Kuroda, S. 2015. Int. J. Nanomedicine 10, 4159–
10 4172.
11 Updyke, T.V., Nicolson, G.L., 1984. J. Immunol. Methods 73, 83–95.
12 Yamada T, Iwabuki H, Kanno T, Tanaka H, Kawai T, Fukuda H, Kondo, A., Seno, M.,
13 Tanizawa, K., Kuroda, S., 2001. Vaccine 19, 3154–3163.

Figure captions

Fig. 1. ZZ-BNC and ZZ-L-membrane (ZZ-L-Mem). (A) Capsular structure of ZZ-BNC. One ZZ-BNC particle consists of ~60 molecules of the ZZ-L protein dimer (~120 molecules of ZZ-L protein monomer) embedded in a lipid bilayer. The ZZ domains could interact with the Fc region. Red cylinders and blue lines indicate ZZ domains and S proteins, respectively. Circle with two bars is phospholipid. Green Y-shaped image is IgG. (B) Preparation of ZZ-BNC-coated and ZZ-L-Mem-coated sensor chip. The ZZ-BNC was adsorbed on the sensor chip and then used for the immobilization of IgGs (upper panels). ZZ-L micelles (ZZ-L-Mic) were prepared by reacting ZZ-BNC with detergent, embedded in LB membrane on sensor chip (ZZ-L-Mem), and then used for the immobilization of IgGs (lower panels).

Fig. 2. Preparation of ZZ-L-Mic. (A and B) AFM topographical images of ZZ-BNC on mica in 3D. ZZ-BNC was treated with or without 5% (w/v) of various detergents (LyEX-MP, NP40, OG, Tween 20, or Tween 80) (A) and 0-5% (w/v) Tween 80 (B). 2D image of 5% Tween 80-treated ZZ-BNC was also shown. Bar, 20 nm. (C) AFM topographical image of ZZ-L-Mic in 2D (left panel). Bar, 20 nm. The size of each small elliptical granule was shown (upper right panel). Postulated structure of ZZ-L-Mic was shown (lower right panel; *see* legend symbols of **Fig. 1A**).

Fig. 3. Preparation of ZZ-L-Mem. (A) AFM topographical images of ZZ-L-Mic on mica in 3D with or without LB membrane (100% DOPC). (B) AFM topographical images (left panels) and phase images (center panels) of ZZ-BNC (upper panels) and ZZ-L-Mem (lower panels) in 2D. Bars, 100 nm. The surface morphology and postulated

structure of ZZ-BNC and ZZ-L-Mem are shown in right panels (*see* legend symbols of **Fig. 1A**). (C) TEM images of ZZ-BNC (upper panels), ZZ-L-Mem (middle panels), and LB membrane (lower panels) with (+) or without (-) 10-nm gold particle-labeled goat total IgG. Bars, 20 nm.

Fig. 4. Optimization of ZZ-L-Mem-coated sensor chip for QCM. (A) Binding capacity of α-actin mouse IgG2a to ZZ-L-Mem consisting of LB membrane (315 ng/cm^2) and various amounts of ZZ-L protein (0-1250 ng/cm^2) on sensor chip. (B) Binding capacity of actin to immobilized α-actin IgG on each ZZ-L-Mem-coated sensor chip. (C) Amounts of bound actin per immobilized α-actin IgG. Bars, standard deviation (n = 3). (D) Repetitive use of ZZ-L-Mem-coated sensor chip. Anti-rabbit total IgG (squares) was injected onto the ZZ-L-Mem-coated sensor chip. After 3-min measurement, the chip was rinsed twice with 0.16 N HCl (arrows) to strip bound IgGs. The cycle of adsorption and removal of IgG was repeated 20 times. Frequency changes in the 1st and 20th cycle are shown in the inset.

Fig. 5. Effect of antibody immobilization on sensitivity and antigen-binding capacity in QCM. (A) Schematic representation of IgGs immobilized onto the bare, ZZ-BNC-coated, and ZZ-L-Mem-coated sensor chips. (B and C) The amounts of bound antigens were calculated from the frequency changes and plotted against the concentrations of injected antigens. (B) Actin and (C) Chicken IgY. White diamonds, bare; black triangles, ZZ-BNC-coated sensor chip; and red circles, ZZ-L-Mem-coated sensor chip. The LOD of the QCM equipment (3 ng/cm^2) is indicated by dashed lines. Data sets used for the analyses are shown with lines for each immobilization method.

Bars, standard deviation (n = 3). (D) Amounts of bound antigen per immobilized IgG. Actin (left panel) and chicken IgY (right panel). White, bare; black, ZZ-BNC-coated sensor chip; and red, ZZ-L-Mem-coated sensor chip. Bars, standard deviation (n = 3).

Fig. 6. Kinetic analyses of antigen-antibody interactions on various sensor chips using SPR. (A) Sensorgrams of α-chicken IgY-chicken IgY interactions on bare, ZZ-BNC-coated, and ZZ-L-Mem-coated sensor chip. The doubling dilution series of chicken IgY (0–500 nM) was injected for 3 min and dissociation monitored for 10 min. The response curves were overlaid and double referenced by subtracting the reference curve signal of a buffer blank. The simple 1:1 kinetic model (red lines) was fitted to each dataset. (B) Association (k_a), dissociation (k_d), and estimated equilibrium dissociation (K_D) constants of α-chicken IgY-immobilized sensor chips.

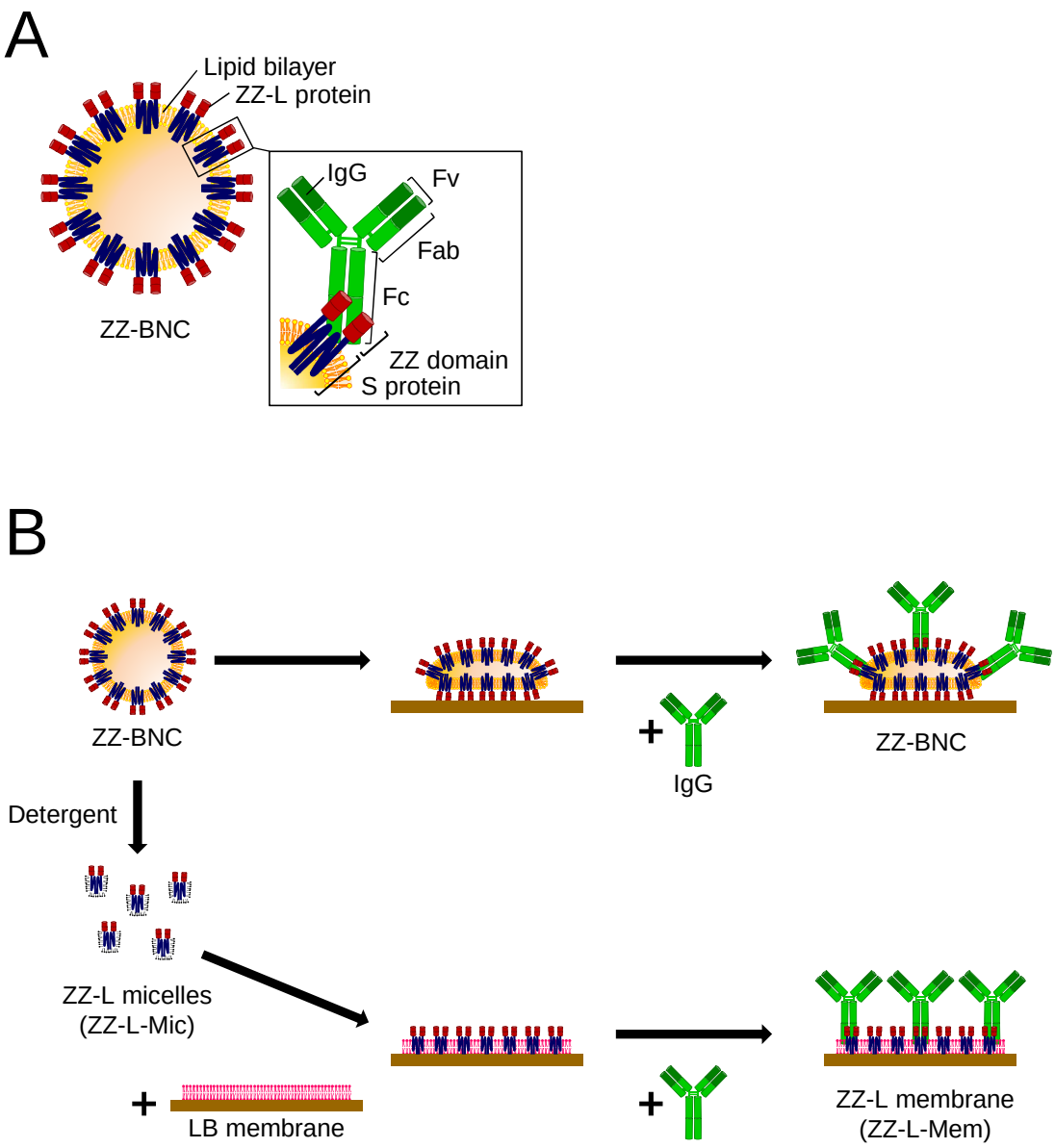

Fig. 1. Iijima et al.

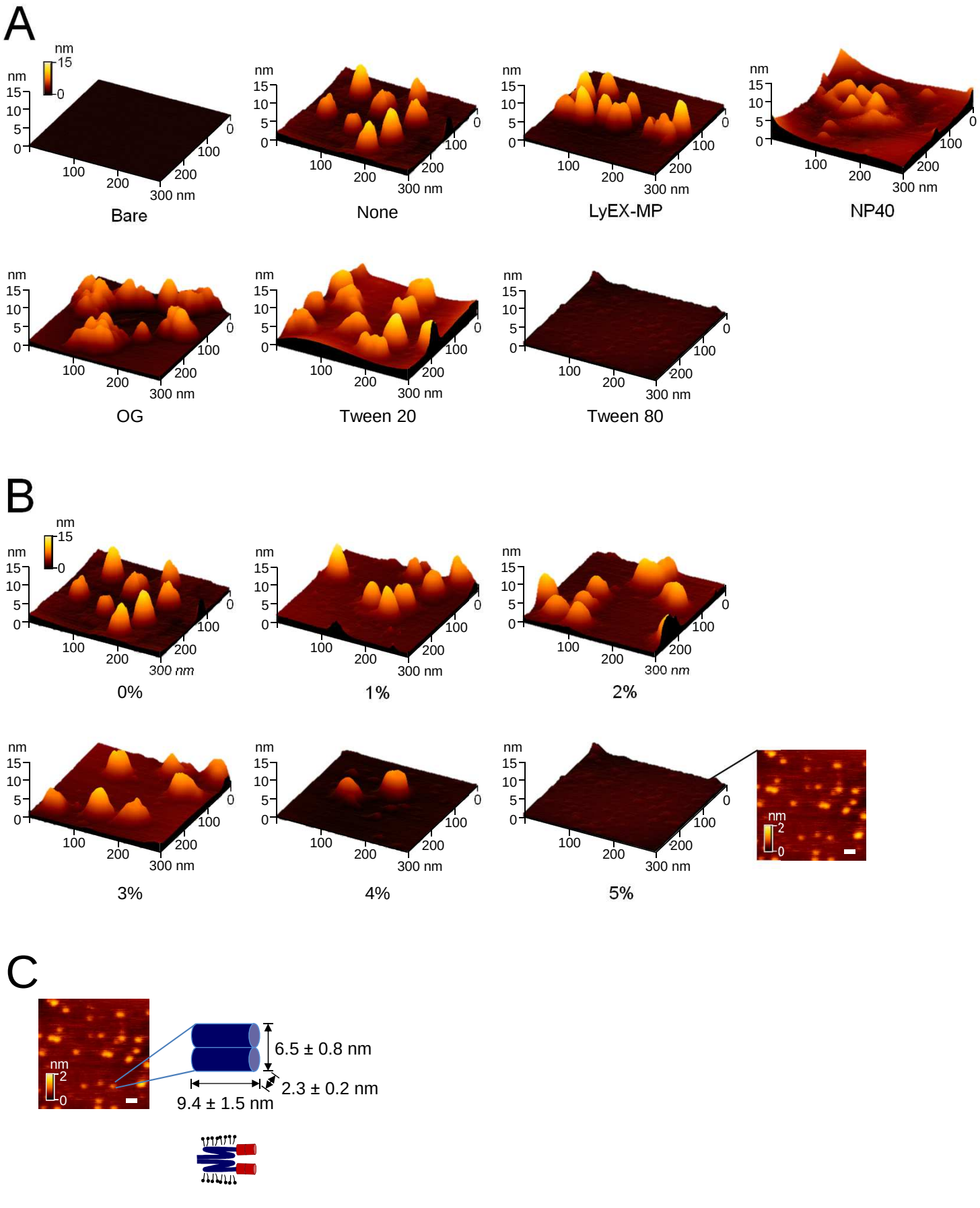

Fig. 2. Iijima et al.

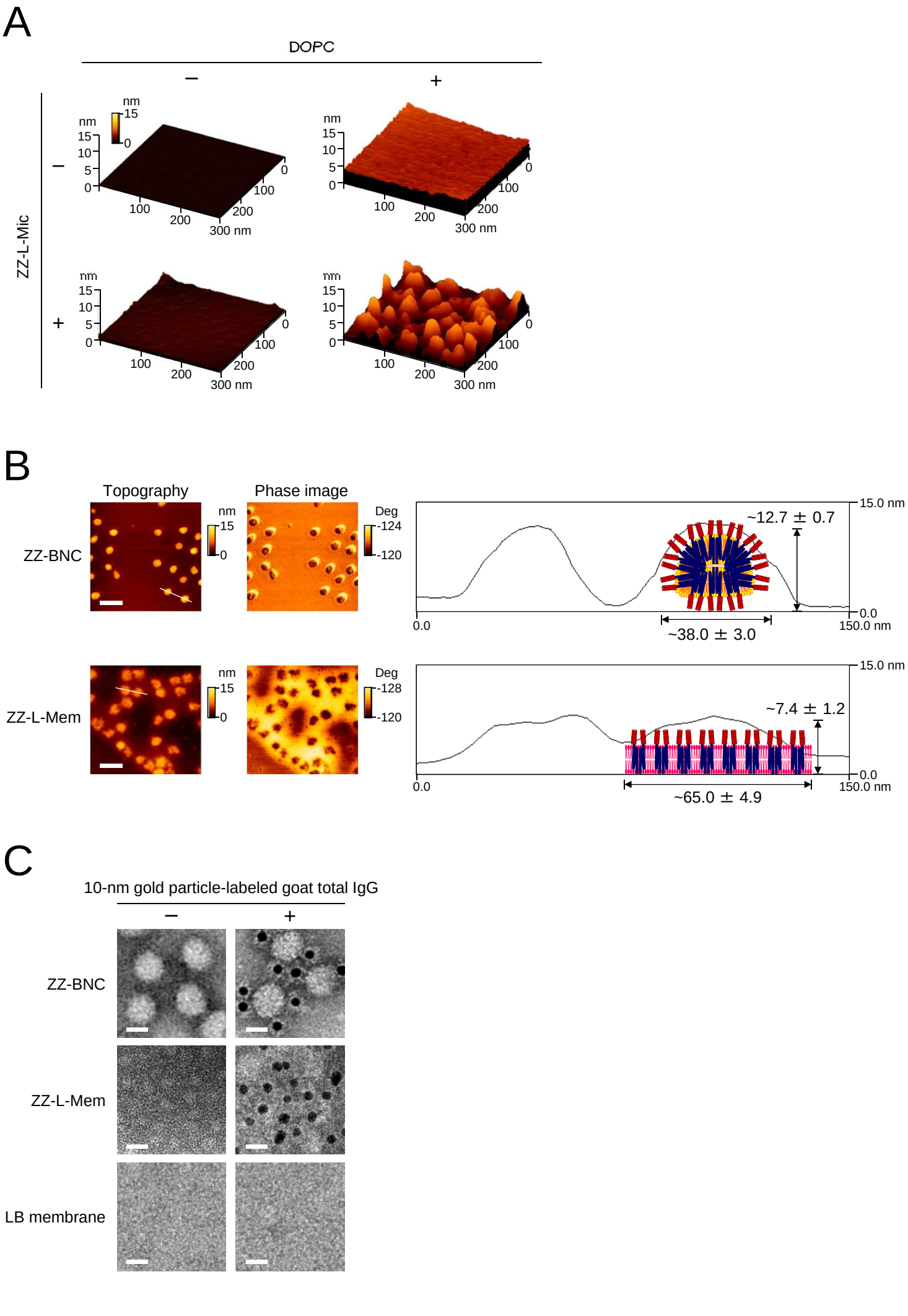

Fig. 3. Iijima et al.

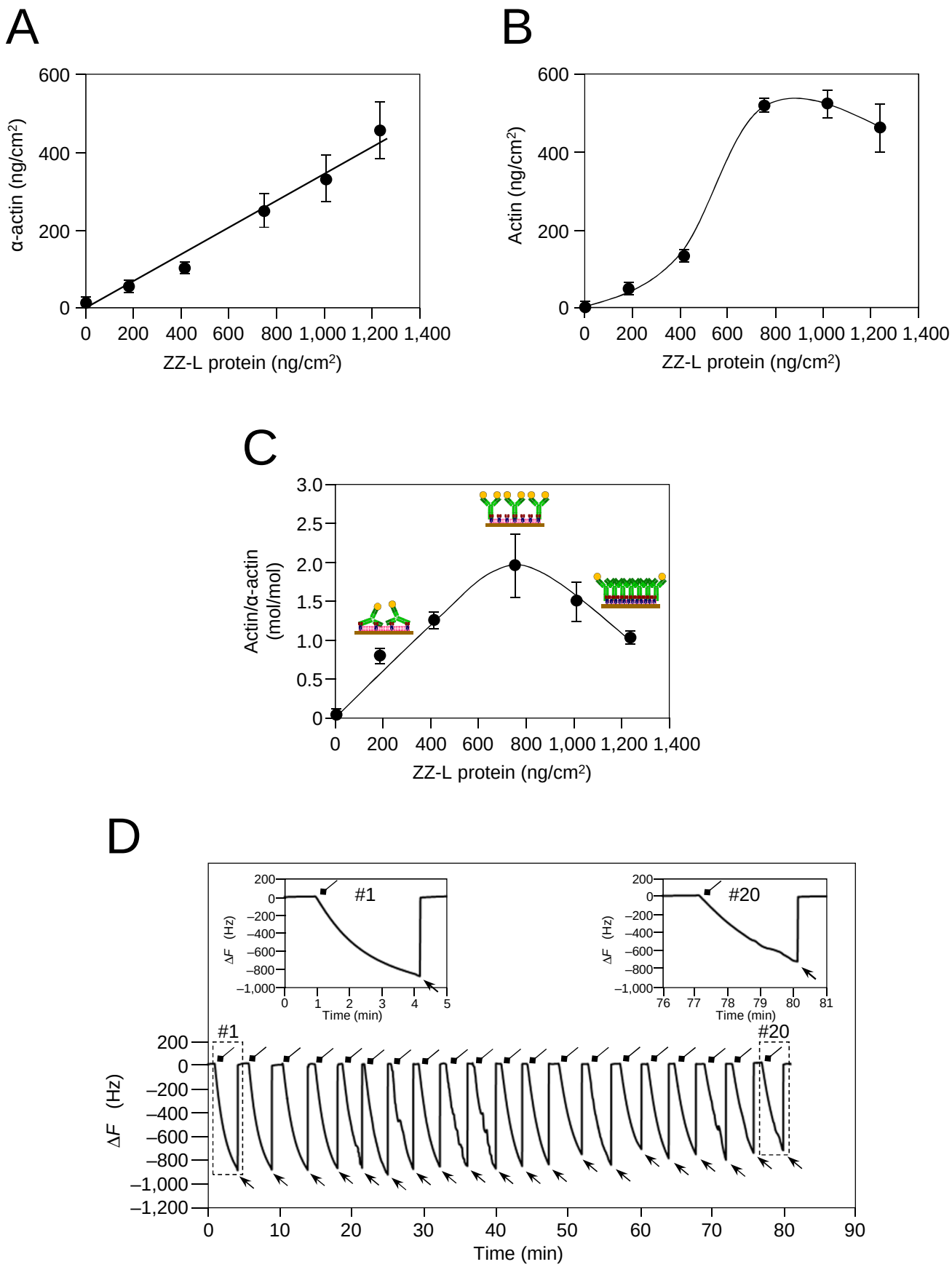

Fig. 4. Iijima et al.

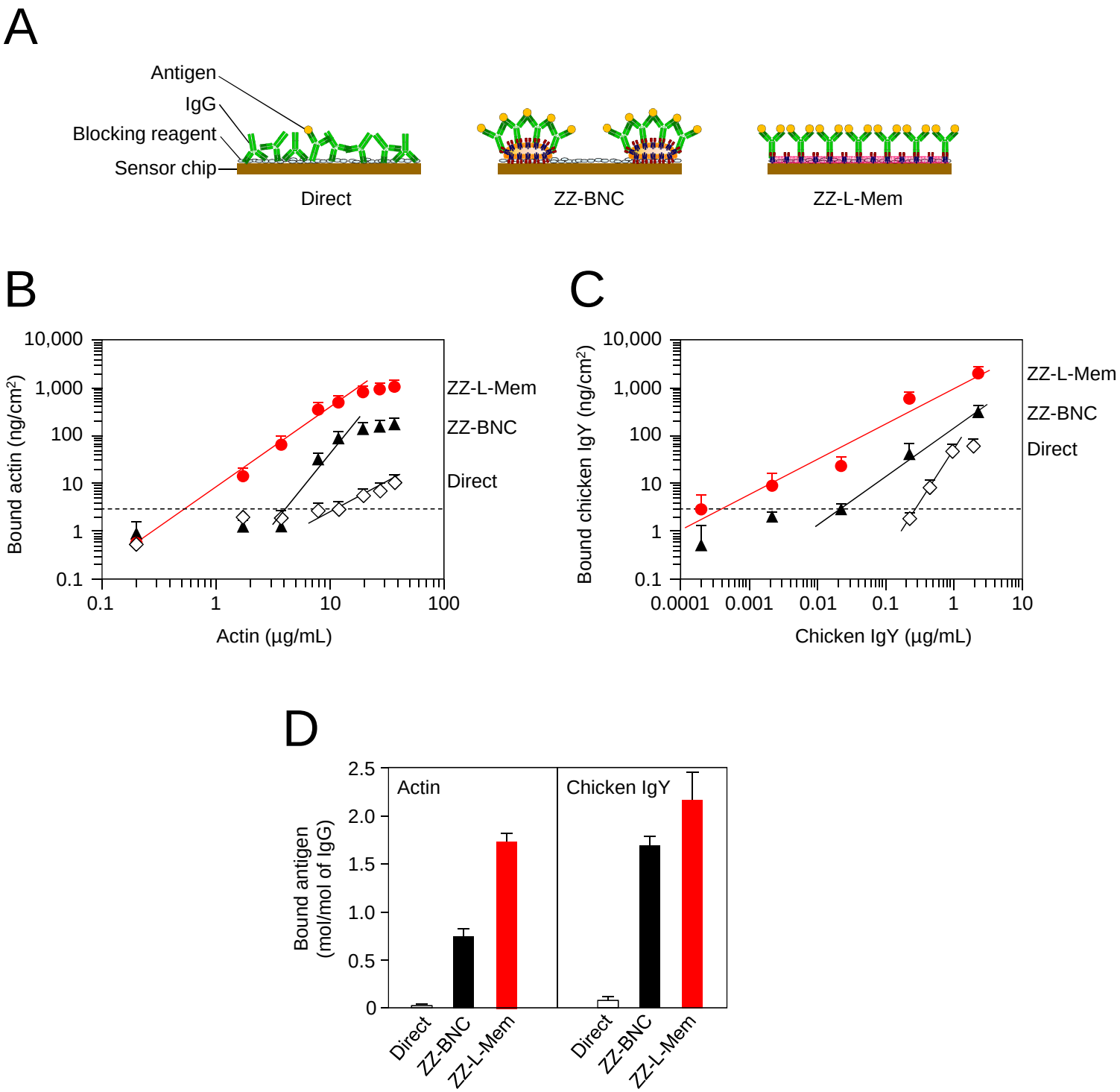

Fig. 5. Iijima et al.

A

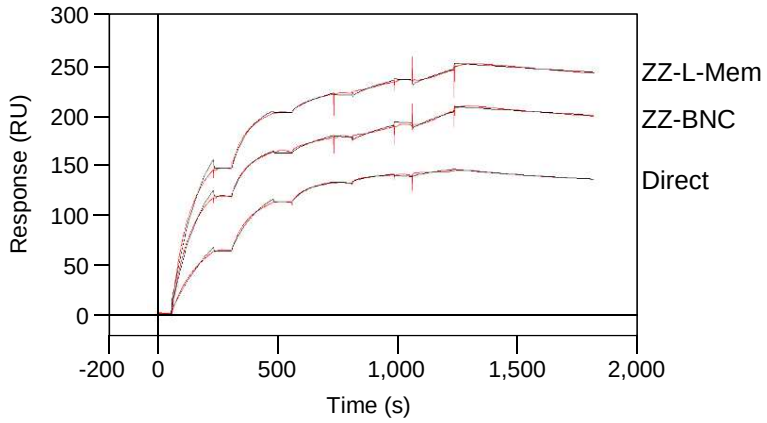

B

α-chicken IgY-immobilized chip	Chicken IgY (analyte)		
	k_a ($M^{-1}s^{-1}$)	k_d (s^{-1})	K_D (M)
Direct	1.01×10^{5}	6.65×10^{-5}	6.58×10^{-10}
ZZ-BNC	1.50×10^{5}	1.78×10^{-6}	1.24×10^{-11}
ZZ-L-Mem	1.44×10^{5}	1.31×10^{-7}	8.78×10^{-13}

Fig. 6. Iijima et al.

Highlights

• ZZ-L membrane could optimize the surface density of ZZ-L proteins on biosensor chip.

• ZZ-L membrane could maximize the antigen-binding capacity of IgGs.

• ZZ-L membrane is a robust scaffold for IgGs on biosensor chip.

• ZZ-L membrane is the most ideal scaffold for the clustering and oriented immobilization of IgGs.

Declaration of interests

☒ The authors declare that they have no known competing financial interests or personal relationships that could have appeared to influence the work reported in this paper.

☐The authors declare the following financial interests/personal relationships which may be considered as potential competing interests: